

World Journal of *Radiology*

World J Radiol 2024 September 28; 16(9): 375-496



EDITORIAL

- 375 Innovative approaches beyond periprocedural hydration for preventing contrast-induced acute kidney injury
Cheng CH, Hao WR, Cheng TH

ORIGINAL ARTICLE**Retrospective Study**

- 380 Intentionally unilateral prostatic artery embolization: Patient selection, technique and potential benefits
Moschouris H, Stamatou K
- 389 Cryoablation of osteoid osteomas: Is it a valid treatment option?
Michailidis A, Panos A, Samoladas E, Dimou G, Mingou G, Kosmoliaptis P, Arvaniti M, Giankoulof C, Petsatodis E
- 398 Radiological findings of February 2023 twin earthquakes-related spine injuries
Bolukçu A, Erdemir AG, İdilman İS, Yıldız AE, Çoban Çifçi G, Onur MR, Akpınar E

Observational Study

- 407 Retinal microcirculation changes in prediabetic patients with short-term increased blood glucose using optical coherence tomography angiography
Hu K, Lv BJ, Zuo HJ, Li QF, Huang FF, Zhang T, Huang RX, Zheng SJ, Wan WJ
- 418 Nomogram for predicting short-term response to anti-vascular endothelial growth factor treatment in neovascular age-related macular degeneration: An observational study
Huang ZH, Tu XZ, Lin Q, Tu M, Lin GC, Zhang KP
- 429 Cerebral perfusion in patients with unilateral internal carotid artery occlusion by dual post-labeling delays arterial spin labeling imaging
Zhang GR, Zhang YY, Liang WB, Ding D

CASE REPORT

- 439 Acquired factor XIII deficiency presenting with multiple intracranial hemorrhages and right hip hematoma: A case report
Wang L, Zhang N, Liang DC, Zhang HL, Lin LQ
- 446 Myelin oligodendrocyte glycoprotein-associated transverse myelitis after SARS-CoV-2 infection: A case report
Zheng JR, Chang JL, Hu J, Lin ZJ, Lin KH, Lu BH, Chen XH, Liu ZG
- 453 Extralobar pulmonary sequestration in children with abdominal pain: Four case reports
Jiang MY, Wang YX, Lu ZW, Zheng YJ

- 460 Behcet's disease-related panuveitis following COVID-19 vaccination: A case report
Lin RT, Liu PK, Chang CW, Cheng KC, Chen KJ, Chang YC
- 466 Hyperparathyroidism presented as multiple pulmonary nodules in hemodialysis patient status post parathyroidectomy: A case report
Chiang PH, Ko KH, Peng YJ, Huang TW, Tang SE
- 473 Secondary rectal linitis plastica caused by prostatic adenocarcinoma - magnetic resonance imaging findings and dissemination pathways: A case report
Labra AA, Schiappacasse G, Cocio RA, Torres JT, González FO, Cristi JA, Schultz M
- 482 *Pneumocystis* pneumonia in stage IIIA lung adenocarcinoma with immune-related acute kidney injury and thoracic radiotherapy: A case report
Zheng YW, Pan JC, Wang JF, Zhang J
- 489 Prolonged course of Paxlovid administration in a centenarian with COVID-19: A case report
Zhang YX, Tang J, Zhu D, Wu CY, Liang ML, Huang YT

ABOUT COVER

Editorial Board Member of *World Journal of Radiology*, Roberto Grassi, MD, Professor, Chief, Department of Radiology, University of Campania Luigi Vanvitelli, Napoli, 80138, Italy. roberto.grassi@unicampania.it

AIMS AND SCOPE

The primary aim of *World Journal of Radiology (WJR, World J Radiol)* is to provide scholars and readers from various fields of radiology with a platform to publish high-quality basic and clinical research articles and communicate their research findings online.

WJR mainly publishes articles reporting research results and findings obtained in the field of radiology and covering a wide range of topics including state of the art information on cardiopulmonary imaging, gastrointestinal imaging, genitourinary imaging, musculoskeletal imaging, neuroradiology/head and neck imaging, nuclear medicine and molecular imaging, pediatric imaging, vascular and interventional radiology, and women's imaging.

INDEXING/ABSTRACTING

The *WJR* is now abstracted and indexed in PubMed, PubMed Central, Emerging Sources Citation Index (Web of Science), Reference Citation Analysis, China Science and Technology Journal Database, and Superstar Journals Database. The 2024 Edition of Journal Citation Reports® cites the 2023 journal impact factor (JIF) for *WJR* as 1.4; JIF without journal self cites: 1.4; 5-year JIF: 1.8; JIF Rank: 132/204 in radiology, nuclear medicine and medical imaging; JIF Quartile: Q3; and 5-year JIF Quartile: Q3.

RESPONSIBLE EDITORS FOR THIS ISSUE

Production Editor: *Wen-Bo Wang*; Production Department Director: *Xu Guo*; Cover Editor: *Jia-Ping Yan*.

NAME OF JOURNAL

World Journal of Radiology

ISSN

ISSN 1949-8470 (online)

LAUNCH DATE

January 31, 2009

FREQUENCY

Monthly

EDITORS-IN-CHIEF

Thomas J Vogl

EDITORIAL BOARD MEMBERS

<https://www.wjgnet.com/1949-8470/editorialboard.htm>

PUBLICATION DATE

September 28, 2024

COPYRIGHT

© 2024 Baishideng Publishing Group Inc

INSTRUCTIONS TO AUTHORS

<https://www.wjgnet.com/bpg/gerinfo/204>

GUIDELINES FOR ETHICS DOCUMENTS

<https://www.wjgnet.com/bpg/GerInfo/287>

GUIDELINES FOR NON-NATIVE SPEAKERS OF ENGLISH

<https://www.wjgnet.com/bpg/gerinfo/240>

PUBLICATION ETHICS

<https://www.wjgnet.com/bpg/GerInfo/288>

PUBLICATION MISCONDUCT

<https://www.wjgnet.com/bpg/gerinfo/208>

ARTICLE PROCESSING CHARGE

<https://www.wjgnet.com/bpg/gerinfo/242>

STEPS FOR SUBMITTING MANUSCRIPTS

<https://www.wjgnet.com/bpg/GerInfo/239>

ONLINE SUBMISSION

<https://www.f6publishing.com>

Observational Study

Nomogram for predicting short-term response to anti-vascular endothelial growth factor treatment in neovascular age-related macular degeneration: An observational study

Zhen-Huan Huang, Xue-Zhao Tu, Qi Lin, Mei Tu, Guo-Cai Lin, Kai-Ping Zhang

Specialty type: Radiology, nuclear medicine and medical imaging**Provenance and peer review:** Unsolicited article; Externally peer reviewed.**Peer-review model:** Single blind**Peer-review report's classification****Scientific Quality:** Grade A**Novelty:** Grade A**Creativity or Innovation:** Grade A**Scientific Significance:** Grade A**P-Reviewer:** Glumac S**Received:** May 7, 2024**Revised:** August 12, 2024**Accepted:** August 14, 2024**Published online:** September 28, 2024**Processing time:** 142 Days and 9.8 Hours**Zhen-Huan Huang, Qi Lin,** Department of Radiology, Longyan First Affiliated Hospital of Fujian Medical University, Longyan 364000, Fujian Province, China**Xue-Zhao Tu,** Department of Orthopedics, Longyan First Affiliated Hospital of Fujian Medical University, Longyan 364000, Fujian Province, China**Mei Tu,** Department of Endocrinology, Longyan First Affiliated Hospital of Fujian Medical University, Longyan 364000, Fujian Province, China**Guo-Cai Lin, Kai-Ping Zhang,** Department of Ophthalmology, Longyan First Affiliated Hospital of Fujian Medical University, Longyan 364000, Fujian Province, China**Corresponding author:** Zhen-Huan Huang, MD, Associate Chief Physician, Department of Radiology, Longyan First Affiliated Hospital of Fujian Medical University, No. 105 North 91 Road, Xinluo District, Longyan 364000, Fujian Province, China. tuxuezhao@163.com

Abstract

BACKGROUND

Anti-vascular endothelial growth factor (anti-VEGF) therapy is critical for managing neovascular age-related macular degeneration (nAMD), but understanding factors influencing treatment efficacy is essential for optimizing patient outcomes.

AIM

To identify the risk factors affecting anti-VEGF treatment efficacy in nAMD and develop a predictive model for short-term response.

METHODS

In this study, 65 eyes of exudative AMD patients after anti-VEGF treatment for ≥ 1 mo were observed using optical coherence tomography angiography. Patients were classified into non-responders ($n = 22$) and responders ($n = 43$). Logistic regression was used to determine independent risk factors for treatment response. A predictive model was created using the Akaike Information Criterion, and its performance was assessed with the area under the receiver operating characteristic curve, calibration curves, and decision curve analysis (DCA) with 500 bootstrap re-samples.

RESULTS

Multivariable logistic regression analysis identified the number of junction voxels [odds ratio = 0.997, 95% confidence interval (CI): 0.993-0.999, $P = 0.010$] as an independent predictor of positive anti-VEGF treatment outcomes. The predictive model incorporating the fractal dimension, number of junction voxels, and longest shortest path, achieved an area under the curve of 0.753 (95%CI: 0.622-0.873). Calibration curves confirmed a high agreement between predicted and actual outcomes, and DCA validated the model's clinical utility.

CONCLUSION

The predictive model effectively forecasts 1-mo therapeutic outcomes for nAMD patients undergoing anti-VEGF therapy, enhancing personalized treatment planning.

Key Words: Vascular endothelial growth factor; Macular degeneration; Neovascularization; Age-related macular degeneration; Choroidal neovascularization; Optical coherence tomography angiography; Nomogram

©The Author(s) 2024. Published by Baishideng Publishing Group Inc. All rights reserved.

Core Tip: This study developed a predictive model using optical coherence tomography angiography to identify factors affecting the effectiveness of anti-vascular endothelial growth factor treatment in neovascular age-related macular degeneration (nAMD). The number of junction voxels emerged as an independent predictor of positive treatment outcomes. Integrating several parameters, the predictive model demonstrated strong performance in forecasting 1-mo therapeutic outcomes, providing a valuable tool for personalized treatment planning in nAMD patients.

Citation: Huang ZH, Tu XZ, Lin Q, Tu M, Lin GC, Zhang KP. Nomogram for predicting short-term response to anti-vascular endothelial growth factor treatment in neovascular age-related macular degeneration: An observational study. *World J Radiol* 2024; 16(9): 418-428

URL: <https://www.wjgnet.com/1949-8470/full/v16/i9/418.htm>

DOI: <https://dx.doi.org/10.4329/wjr.v16.i9.418>

INTRODUCTION

The global rise in the incidence of age-related macular degeneration (AMD)[1,2] is emerging as the primary cause of irreversible vision loss in individuals aged 50 and above. Neovascular AMD (nAMD) is a particularly severe form that can result in blindness if not adequately treated[3,4]. The intravitreal administration of anti-vascular endothelial growth factor (anti-VEGF) agents is emerging as the primary therapeutic approach[5], substantially improving the condition of eyes with nAMD. The response to this therapy is suboptimal in many patients, as they often experience persistent intraretinal, subretinal, or subretinal pigment epithelial fluid and ongoing or new hemorrhages, along with progressive lesion fibrosis[6].

To customize treatment plans, clinicians often prioritize reducing exudative symptoms such as intraretinal cystoid fluid, subretinal fluid, and fluid or hemorrhage beneath the retinal pigment epithelium (RPE) layer[7]. These approaches often vary significantly among patients due to differences in baseline clinical characteristics and choroidal neovascularization (CNV) lesions[8]. Optical coherence tomography angiography (OCTA) provides a non-invasive, high-resolution imaging technique that offers both qualitative and quantitative assessment of CNV[9]. While OCTA-measured CNV parameters, such as the growth of macular neovascularization (MNV)[10], vessel junction density[11], the change in most excellent vascular caliber[12], and vessel density[1], have demonstrated effectiveness in monitoring changes in CNV due to anti-VEGF therapy, the ability of these parameters to predict treatment outcomes remains a topic of ongoing debate.

Considering the complexities and diverse responses to anti-VEGF therapy among individuals, the primary objective of this study was to identify potential biomarkers that can predict treatment response in nAMD patients following anti-VEGF therapy based on baseline clinical characteristics and OCTA-measured parameters. Subsequently, we constructed a predictive model through logistic regression analysis and filtered variables based on the Akaike Information Criterion (AIC) to develop individualized, precision-based treatment plans, thereby maximizing the efficacy of nAMD interventions and potentially improving the quality of life for affected individuals.

MATERIALS AND METHODS

Participants

The study received approval from the Medical Ethics Committee of our hospital and followed the principles outlined in the Declaration of Helsinki. Written consent was not required due to the retrospective nature of the study. Eighty-three patients with unilateral nAMD who had not undergone any prior treatment were included in this study. They were

followed up for at least 1 mo using OCTA from January 2020 to September 2023. However, 18 patients were excluded based on the following exclusion criteria: (1) nAMD with prior anti-VEGF injection treatment or intraocular surgery other than cataract surgery ($n = 9$); (2) Lack of clinical history ($n = 1$); (3) Absence of follow-up using OCTA for at least 1 mo ($n = 1$); (4) Poor-quality images obtained by OCTA ($n = 2$); and (5) Macular neovascularization caused by high myopia (≥ -6.00 diopters), glaucoma, diabetic retinopathy, uveitis, or endophthalmitis ($n = 5$). Consequently, the study comprised 65 eyes from 65 eligible patients (20 females and 45 males; median age: 68 years; age range: 51-87 years) experiencing unilateral nAMD. A flow chart of the enrollment process is shown in [Figure 1](#).

Grouping of response to antiVEGF therapies

Three initial loading doses of intravitreal anti-VEGF injections were administered for treatment-naïve eyes with exudative AMD, followed by achieving the first remission, defined as a dry macula on optical coherence tomography. Once remission was achieved, a *pro re nata* or treat-and-extend regimen was implemented for recurrent exudation.

Patients were classified into response and non-response groups according to their OCTA follow-up outcomes after a month-long loading phase of anti-VEGF therapy. Specifically, the response group comprised 43 individuals, while the non-response group included 22. According to the criteria established by Amoaku *et al*[8], patients in the response group demonstrated an improvement in visual acuity of ≥ 5 ETDRS letters, a reduction in central retinal thickness of $> 25\%$, or a decrease in subretinal or intraretinal fluid and cysts. In the non-response group, patients failed to meet these criteria. In case of classification disagreements between two evaluators, a third evaluator was consulted to reach a consensus.

Collection of clinical data and analysis of OCTA imaging features

The hospital's electronic medical record management system was utilized to systematically collect comprehensive clinical data of patients, including information on age, gender, hypertension, diabetes mellitus, alcohol consumption, and smoking habits. CNV lesions were captured using a high-quality 3 mm \times 3 mm OCTA scanning device (Heidelberg Engineering, Heidelberg Germany) at baseline and during each subsequent visit. The OCTA device's built-in software automatically segmented the en-face images of the CNV complex based on two horizontal lines extending from the inner plexiform layer/inner nuclear layer to enhance visualization.

The morphology of the CNV complex was classified as ([Figure 2](#)): (1) "Medusa" or "sea fan," which is characterized by central feeder vessels with main vascular trunks and numerous tiny capillaries radiating from the center; (2) "Long linear vessels," which lack prominent capillary ramifications; and (3) "Indistinct network," which is defined by the visualization of only main vascular trunks and thin branches without detectable feeder vessels. Quantitative features of the CNV, including area, fractal dimension, branch number, junction number, the number of end-point voxels, the number of junction voxels, the number of slab voxels, average branch length, maximum branch length, and longest shortest path, were assessed using ImageJ software on the segmented OCTA images. Two masked retina specialists independently evaluated both qualitative and quantitative parameters. In cases of interpretive disagreement, a consensus was reached through open adjudication involving others.

Predictive model construction

Using univariate and multivariate logistic regression analyses, clinical data and OCTA imaging characteristics were collected to identify independent risk factors associated with the response of patients diagnosed with nAMD following anti-VEGF therapy. Odds ratios (OR) and 95% confidence intervals (CI) were employed as effect measures. Variables demonstrating a P value < 0.2 in the univariate logistic regression analysis were included in subsequent multivariate logistic regression analysis, which was further refined based on AIC for selection. AIC measures goodness-of-fit for statistical models, selecting the model that best interprets data while containing minimal free parameters among n models. For predictive model construction, the multivariate logistic regression analysis included variables selected through AIC refinement, with all identified variables entered into the regression equation.

The discrimination efficacy of the predictive model was assessed by calculating the area under the receiver operating characteristic (ROC) curve (AUC) using 500 bootstrap re-samples. The DeLong test was used to compare AUC values among different models. In addition, integrated discrimination improvement (IDI) was used to measure how much better average sensitivity was compared to other models while maintaining average specificity. The agreement between predicted outcomes from predictive models and actual responses was evaluated using calibration plots with 500 bootstrap re-samples and the Hosmer-Lemeshow test's application. Decision curve analysis (DCA) with 500 bootstrap re-samples was conducted to examine this predictive model's clinical utility and effectiveness.

Statistical analysis

The statistical analyses were conducted utilizing IBM SPSS Statistics 22 software and R software (version 4.2.0). A two-tailed P value < 0.05 was considered statistically significant. Continuous variables are described as the mean \pm SD or median with interquartile range, and group comparisons were made using the Student's t -test or Wilcoxon test. Categorical variables are presented as counts and percentages, with group comparisons performed using the χ^2 test or Fisher's exact test. The sample size estimation was based on the multivariate regression analysis requirements, where the recommended sample size is 15 to 20 times the number of variables. The sample size was increased by 10% to account for potential data loss.

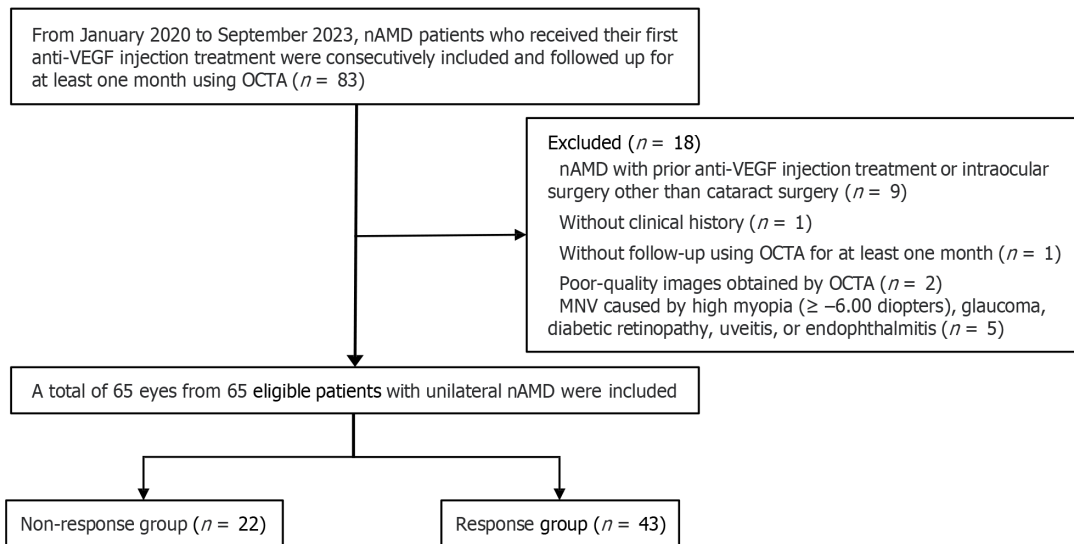


Figure 1 Flowchart of study cohort selection. nAMD: Neovascular age-related macular degeneration; anti-VEGF: Anti-vascular endothelial growth factor; OCTA: Optical coherence tomography angiography.

RESULTS

Clinical and OCTA characteristics of the study cohort

The age and gender distributions did not differ significantly between the non-response and response groups ($P = 0.792$ and 0.878 , respectively). Personal and medical histories, including smoking habits, alcohol consumption, hypertension, and diabetes mellitus, also showed no statistically significant disparities ($P = 0.378$ - 1.000). No significant variations were observed in the morphology of the CNV complex between the non-response and response groups ($P = 1.000$). The baseline quantitative features of the CNV demonstrated no substantial discrepancies between the non-response and response groups ($P = 0.050$ - 0.368).

Risk factors related to response to antiVEGF therapies

Univariate and multivariate logistic analyses were conducted to identify independent risk factors associated with the response to anti-VEGF agents, as presented in [Table 1](#). Variables with a P value < 0.2 in the univariate logistic regression analysis, including fractal dimension, branch number, junction number, and the number of junction voxels, were further screened using multivariate logistic regression analysis, which demonstrated a significant correlation between the response to anti-VEGF therapies and the number of junction voxels (OR = 0.997, 95% CI: 0.993-0.999, $P = 0.010$).

Performance of the predictive model

The predictive model, depicted by a nomogram in [Figure 3](#), used AIC to screen variables and ultimately included fractal dimension, the number of junction voxels, and the longest shortest path ([Figure 4](#)). Mathematically represented as $Y = 31.901 - 16.294 \times \text{fractal dimension} - 0.002 \times \text{the number of junction voxels} + 0.003 \times \text{the longest shortest path}$, this model enables precise evaluation of treatment on the risks and probabilities of adverse response. The discriminatory capacity of the predictive model was evaluated using a ROC curve. The pooled AUC (95% CI) of 0.753 (0.622-0.873) demonstrates a moderately good performance for the predictive model ([Figure 5A](#) and [B](#)). The predictive model showed an accuracy of 0.723 (95% CI: 0.717-0.729), a sensitivity of 0.744 (95% CI = 0.614-0.875), and a specificity of 0.682 (95% CI = 0.487-0.876) at a threshold value of 0.709. [Figure 5C](#) shows that the AUC values of the variables screened using AIC were not statistically different from the AUC of the nomogram ($P = 0.078$ for fractal dimension *vs* nomogram, $P = 0.181$ for the number of junction voxels *vs* nomogram, and $P = 0.083$ for the longest shortest path *vs* nomogram).

The inclusion of fractal dimension [IDI (95% CI) = 0.613 (0.059-0.267), $P = 0.002$], the number of junction voxels [IDI (95% CI) = 0.136 (0.049-0.223), $P = 0.002$], and the longest shortest path [IDI (95% CI) = 0.204 (0.089-0.319), $P = 0.001$] significantly enhanced the predictive value of the model compared to variables selected using AIC. The calibration curves of the nomogram ([Figure 5D](#)), based on 500 bootstrap re-samples, demonstrated a significant correlation between the predicted probability by the model and the reference line (Hosmer-Lemeshow test: $\chi^2 = 7.320$ $P = 0.604$), indicating robust alignment. [Figure 5E](#) shows the calibration curves of different models for predicting anti-VEGF therapy response. The application of DCA has demonstrated the potential to enhance net benefits and exhibit a diverse range of threshold probabilities ([Figure 5F](#) and [G](#)).

Table 1 Univariate and multivariate analyses of clinical and optical coherence tomography angiography characteristics associated with response to anti-vascular endothelial growth factor therapy

Characteristic	Univariate		Multivariate	
	OR (95%CI)	P value	OR (95%CI)	P value
Age (years)	0.997 (0.947-1.049)	0.901		
Gender (male)	0.777 (0.237-2.356)	0.663		
Hypertension	1.920 (0.649-6.229)	0.252		
Diabetes mellitus	0.650 (0.13-3.571)	0.596		
Smoking habits (active and former smoker)	0.602 (0.198-1.852)	0.368		
Alcohol consumption (active and former drinker)	0.917 (0.292-3.072)	0.883		
Morphological feature (long linear vessels)	1.029 (0.190-5.409)	0.973		
Morphological feature (indistinct network)	1.187 (0.271-4.694)	0.810		
Area (mm ²)	0.448 (0.053-3.733)	0.444		
Fractal dimension	0.000 (0.000-6.103)	0.093	0.000 (0.000-486.4)	0.195
Branch number	0.999 (0.998-1.000)	0.171	1.004 (0.995-1.014)	0.362
Junction number	0.997 (0.991-1.001)	0.179	1.013 (0.977-1.056)	0.489
Number of end-point voxels	1.000 (0.999-1.001)	0.517		
Number of junction voxels	0.999 (0.999-1.000)	0.047	0.997 (0.993-0.999)	0.010
Number of slab voxels	1.000 (0.999-1.000)	0.214		
Average branch length (mm)	1.000 (0.998-1.001)	0.601		
Maximum branch length (mm)	1.000 (0.999-1.001)	0.575		
Longest shortest path (mm)	1.000 (0.999-1.000)	0.555		

OR: Odds ratio; CI: Confidence interval.

DISCUSSION

This study identified the number of junction voxels as a critical predictor of positive treatment outcomes in patients with nAMD undergoing anti-VEGF therapy. The developed predictive model, incorporating the fractal dimension, number of junction voxels, and longest shortest path, demonstrated high accuracy in forecasting 1-mo therapeutic responses. This model offers a valuable tool for personalized treatment planning in nAMD patients.

There is significant inter-individual variability in terms of disease progression and response to anti-VEGF therapy among patients with nAMD. Consequently, the challenge lies in tailoring precise, individualized treatment for each patient. Even though qualitative analysis of morphological CNV findings using OCTA can offer direct insights into the disease stage and activity status of CNV and hold clinical significance for treatment and prognosis[13-16], its application in clinical practice is subject to significant limitations. Indeed, our study revealed no significant correlation between the morphology of CNV on OCTA and the response to anti-VEGF treatment. Therefore, this study aimed to assess the vascular architecture of CNV using quantitative OCTA parameters at baseline to identify potential predictors of treatment response. Subsequently, this study aimed to construct a predictive model that provides insights into the risks and probabilities of adverse responses 1 mo after treatment.

The present study aimed to develop and evaluate a nomogram that integrates fractal dimension, the number of junction voxels, and the longest shortest path for predicting response to anti-VEGF therapy. Our comprehensive evaluation, encompassing ROC analysis, calibration curve assessment, and DCA, demonstrated satisfactory predictive accuracy and discriminative ability.

The fractal dimension represents a geometric index that delineates the complexity of vascular anatomy (normal range: 0-2; a higher fractal dimension value indicates a more complex vascular network structure). Al-Sheikh *et al*[13] postulated that active CNV had a higher fractal dimension. Similar results were reported by Faatz *et al*[17], suggesting that the fractal dimension serves as a valuable parameter for assessing the activity of CNV, with a higher fractal dimension being positively associated with increased CNV activity. Furthermore, they concluded that the baseline fractal dimension of CNV can serve as a predictive factor for the response to anti-VEGF therapy. However, Coscas *et al*[16] showed conflicting results, suggesting that active CNV had a lower fractal dimension. A study conducted by Serra *et al*[18] also showcased that the fractal dimension could be helpful in objectively assessing the activity status of CNV and highlighted that a significantly lower fractal dimension characterized active CNV. As previously hypothesized by Carnevali *et al*[19], the fractal dimension was associated with the absence of core vessels, which likely indicates a more complex vascular

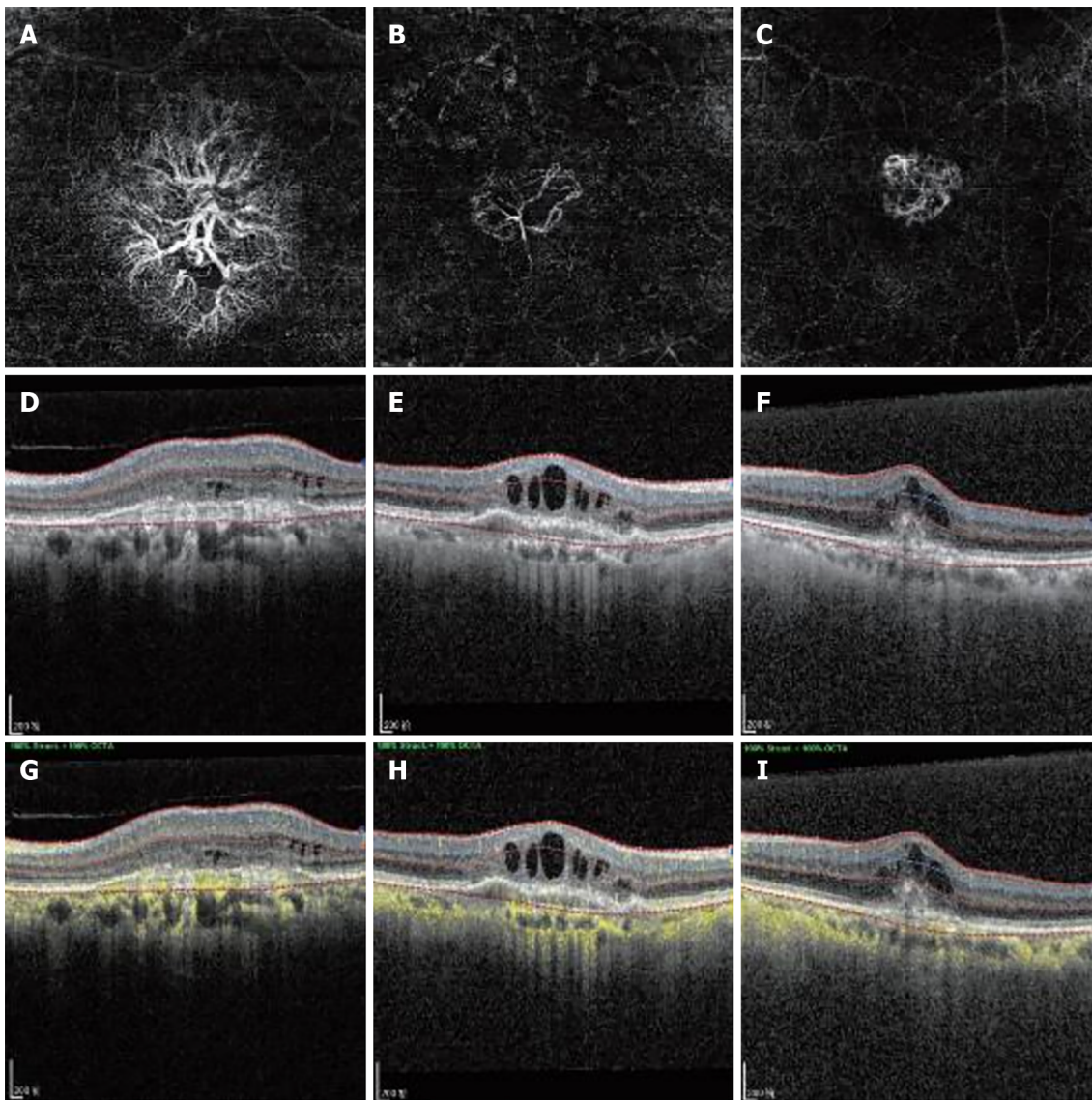


Figure 2 Morphological findings of choroidal neovascularization evaluated through qualitative analysis of optical coherence tomography angiography. A: A 51-year-old female patient with a "medusa" or "sea fan" pattern of choroidal neovascularization (CNV) in the oculus sinister; B: An 85-year-old male patient with a "long linear vessels" pattern of CNV in the oculus dexter; C: A 65-year-old female patient with an "indistinct network" pattern of CNV in the oculus sinister; D-F: Corresponding B-scan images showing the segmentation lines; G-I: Corresponding B-scan images with flow signals.

structure and may be considered a protective factor against exudative activity, thereby enhancing the effectiveness of anti-VEGF therapy. The fractal dimension was identified as a significant predictor in our study's univariate logistic regression analysis; however, it did not demonstrate independent significance as a risk factor for predicting response to anti-VEGF therapy in the multivariate logistic regression analysis, contrary to findings from previous studies. Different studies have yielded partially inconsistent results, which may be attributed to variations in sample size or discrepancies between observers across various studies. Although fractal dimension was not a significant predictor in multivariate logistic regression analysis, the final predictive model had the best diagnostic performance when it was included in the model.

The OCTA images of type 1 CNV have been previously described as exhibiting "sea fan," "medusa," or "tangled" patterns[20,21], while type 2 CNV has been characterized by a branching network of densely packed smaller caliber vessels radiating from the main trunk with a distinct demarcation[22,23]. The study by Suzuki *et al*[24] revealed that patients with type 1 CNV tend to develop resistance to anti-VEGF therapy, which can be attributed, at least partially, to the preserved barrier function of the RPE, impeding the rapid penetration of anti-VEGF drugs. The study conducted by Nakano *et al*[11], demonstrated that the mean vessel junction density of type 2 CNVs ($8.69 \pm 2.05/\text{mm}$) was significantly higher than that of type 1 CNVs ($7.30 \pm 2.40/\text{mm}$, $P = 0.008$). This finding suggested that type 1 CNVs exhibited a more significant presence of mature vessels and indicated their potential resistance against anti-VEGF therapy. Therefore, it could be inferred that vessel maturation contributed to the anti-VEGF resistance observed in type 1 CNVs. In line with this assumption, the study conducted by Kuehlewein *et al*[25] observed a higher incidence of large mature neovascular complexes in eyes with type 1 CNV compared to those with type 2 CNV, indicating an increased likelihood of poor responses to anti-VEGF treatment. Similarly, Jia *et al*[12] and Mettu *et al*[6] have identified that the specific subtype of

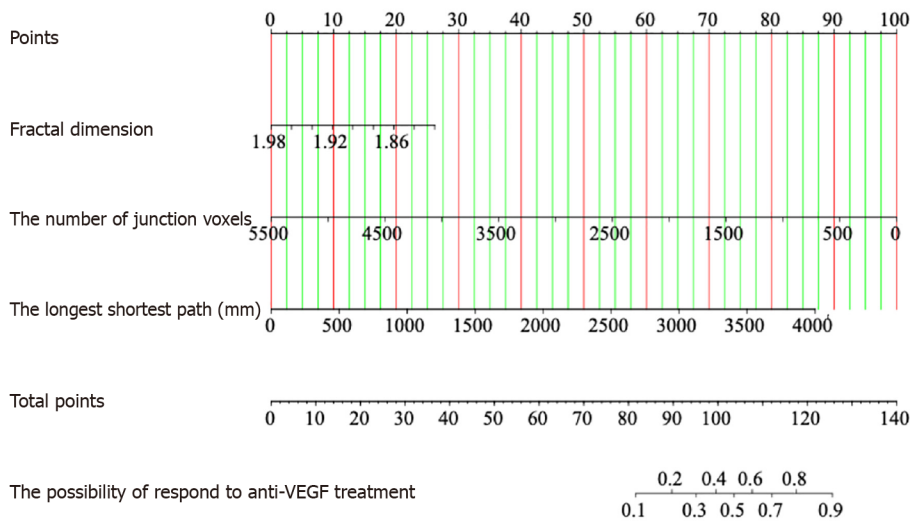


Figure 3 The constructed nomogram for predicting response to anti-vascular endothelial growth factor therapy. VEGF: Vascular endothelial growth factor.

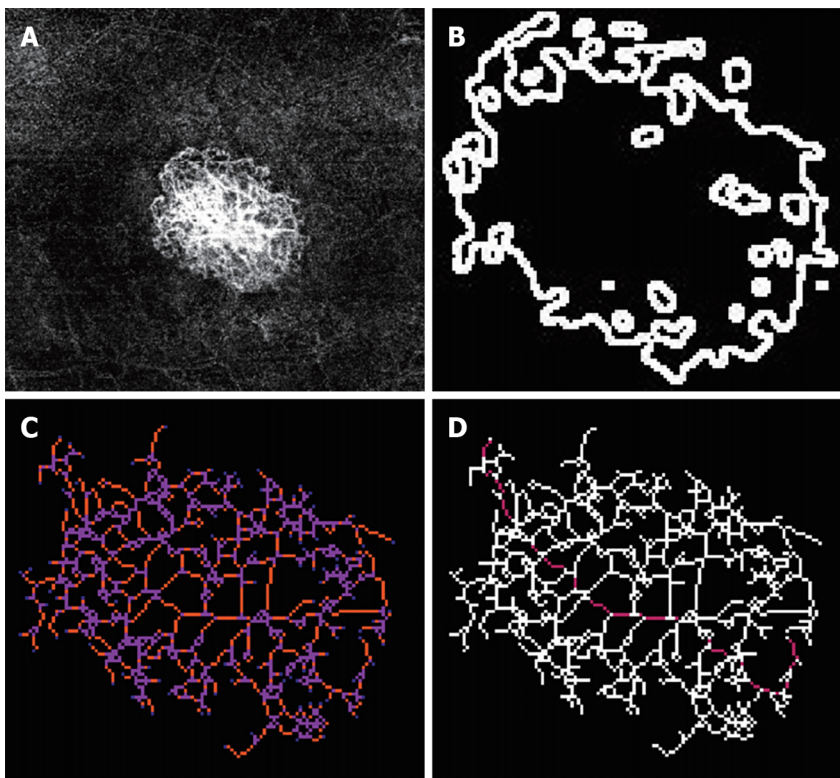


Figure 4 A 74-year-old female patient with an "indistinct network" pattern of choroidal neovascularization in the oculus dexter. A: 3 mm × 3 mm en-face optical coherence tomography angiography image showing the dense small vessels after removal of projection artifacts; B: Corresponding en-face choriocapillaris images were imported into ImageJ software for quantitative measurement of choroidal neovascularization parameters, including fractal dimension; C: End-point voxels in blue, slab voxels in orange, and junction voxels in purple; D: Longest shortest path in red.

CNV was significantly associated with the response to anti-VEGF therapy, suggesting that type 2 CNV exhibited a more favorable response to anti-VEGF treatment. Nevertheless, the response to long-term treatment may vary, particularly in cases of type 2 CNV. Daniel *et al*[26] and Daniel *et al*[27] revealed that patients with type 2 CNV exhibited an elevated risk of experiencing a suboptimal response to anti-VEGF therapy after five years of treatment compared to patients with other CNV subtypes, regardless of the specific drug or treatment regimen employed.

Three-dimensional skeletonization has been developed as an ImageJ plugin[28]; the plugin performs voxel segmentation in a skeleton image, accurately identifying junctions, triple and quadruple points, and branches while measuring their average and maximum length. Each voxel is classified into one of three types based on its neighboring voxels: (1) End-point voxels with less than two neighbors; (2) Junction voxels with more than two neighbors; and (3) Slab

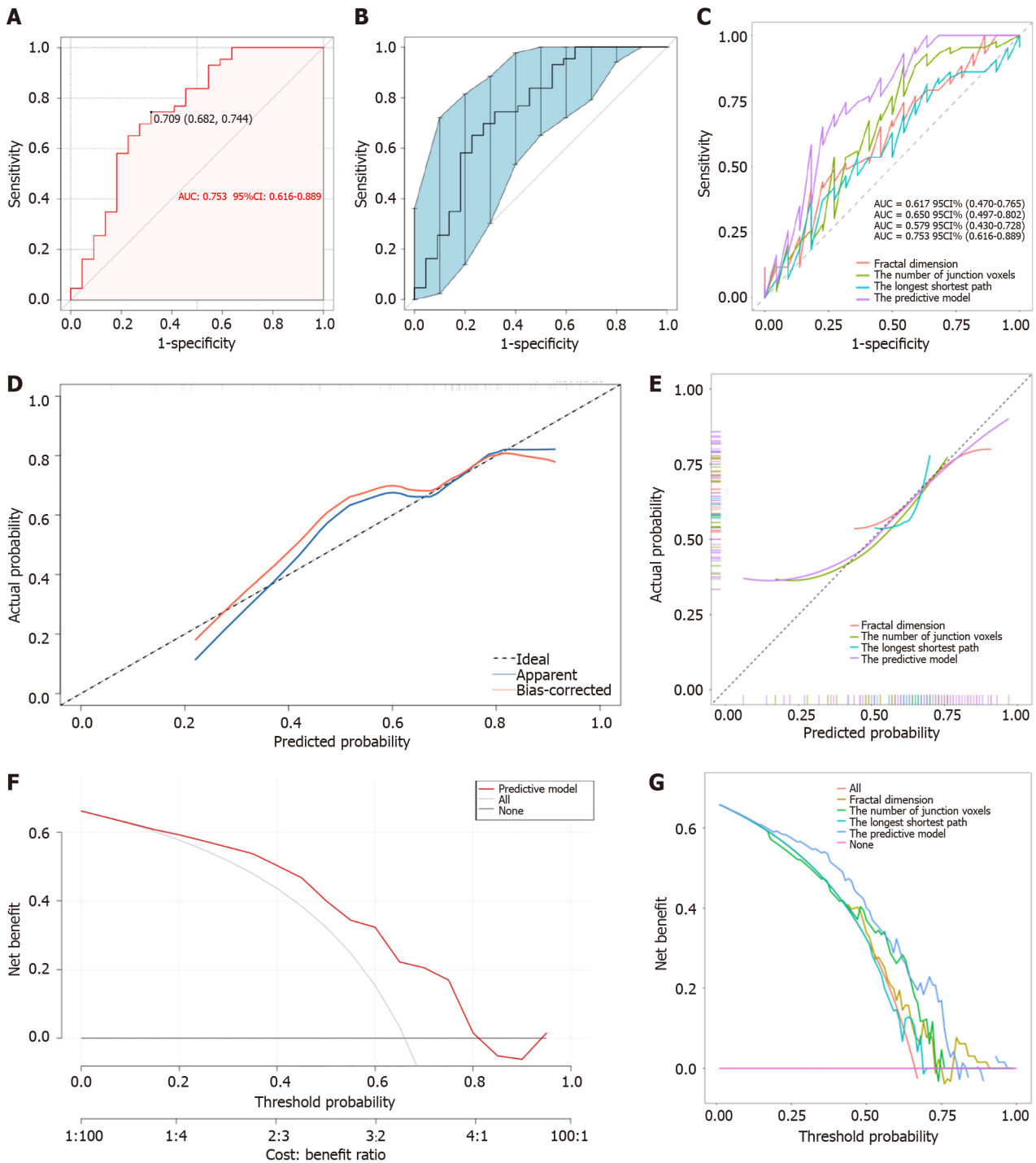


Figure 5 Area under the receiver operating characteristic curve, calibration curve, and decision curve analysis for the model predicting anti-vascular endothelial growth factor therapy response. A: Receiver operating characteristic (ROC) curve for the predictive model; B: ROC curves based on 500 bootstrap re-samples; C: ROC curves comparing different models; D: Calibration curves based on 500 bootstrap re-samples; E: Calibration curves comparing different models; F: Decision curve analysis based on 500 bootstrap re-samples; G: Decision curve analysis comparing different models.

voxels with precisely two neighbors. The resulting classifications are displayed in a new window, where a unique color represents each classification. Note that, according to this notation, the number of junction voxels may differ from the number of junctions due to potential voxel adjacency. Despite previous studies explaining the seemingly superior anti-VEGF responses in type 2 CNV cases, controversy remains. Our research not only observed an independent association between the number of junction voxels and predicting anti-VEGF response but also discovered that eyes with fewer junction voxels were more likely to exhibit a favorable response to anti-VEGF therapy, aligning with Daniel *et al*'s and Daniel *et al*'s findings suggesting poor anti-VEGF response in type 2 CNV cases characterized by dense vessel branching networks[26,27]. The variation in follow-up duration may account for the difference from most previous studies.

Although this study's univariate and multivariate analyses showed that the longest shortest path was not a significant and independent risk factor for anti-VEGF response, this study included the longest shortest path in the final prediction

model according to AIC screening variables. To our knowledge, the longest shortest path refers to the maximum distance that the shortest paths within the skeleton can cover in skeletal structure analysis. By comparing the longest and shortest paths of skeletal structures in different images, researchers can identify which structures are larger, more complex, or more interconnected. The longest shortest path offers information about the size and extent of the skeletal structure, with longer shortest paths typically indicating larger structures or longer branches. Complex structures often exhibit longer shortest paths due to multiple branches and junctions. If the shortest path is exceptionally long, it may indicate that certain parts of the structure are not interconnected through short paths, potentially indicating isolated or separate regions within the structure.

Our study has some limitations. On the one hand, the single-center study with a limited sample size had inherent selection biases. In order to mitigate this concern, we conducted 500 bootstrap re-samples to generate additional virtual samples from the original dataset, thereby increasing the sample size and mitigating the impact of sampling bias on the statistical power of the analysis. On the other hand, external data have not validated the risk prediction model, and its generalization performance remains unclear. Therefore, future studies should include external validation using larger datasets from other centers that can reliably predict outcomes.

CONCLUSION

In summary, the findings of our study suggest that the number of junction voxels is an independent predictor of the response to anti-VEGF therapy. The predictive model was established in combination with OCTA-measured parameters of CNV vascular architecture (including fractal dimension, the number of junction voxels, and the longest shortest path), demonstrating moderately good predictive efficacy and can assist clinicians in selecting individualized treatment for nAMD by predicting outcomes.

FOOTNOTES

Author contributions: Huang ZH and Lin GC conceived and designed the study; Huang ZH, Zhang KP, and Tu XZ collected and assembled the data; Huang ZH, Tu XZ, Lin Q, and Tu M analyzed and interpreted the data. All authors have read and approved the final manuscript.

Supported by Fujian Province Natural Science Foundation of China, No. 2020J011321.

Institutional review board statement: The study was reviewed and approved by the Longyan First Affiliated Hospital of Fujian Medical University (approval No. 202014).

Informed consent statement: As this retrospective observational study used anonymous clinical data from patients who have already consented to treatment, no additional consent was needed. Patients were informed of potential research use at the time of treatment consent.

Conflict-of-interest statement: There are no conflicts of interest to report.

Data sharing statement: The datasets generated and analyzed during the current study are available from the corresponding author on reasonable request.

STROBE statement: The authors have read the STROBE Statement-checklist of items, and the manuscript was prepared and revised according to the STROBE Statement-checklist of items.

Open-Access: This article is an open-access article that was selected by an in-house editor and fully peer-reviewed by external reviewers. It is distributed in accordance with the Creative Commons Attribution NonCommercial (CC BY-NC 4.0) license, which permits others to distribute, remix, adapt, build upon this work non-commercially, and license their derivative works on different terms, provided the original work is properly cited and the use is non-commercial. See: <https://creativecommons.org/licenses/by-nc/4.0/>

Country of origin: China

ORCID number: Zhen-Huan Huang 0000-0002-2472-3102.

S-Editor: Qu XL

L-Editor: Wang TQ

P-Editor: Yu HG

REFERENCES

- 1 Hsu CR, Lai TT, Hsieh YT, Ho TC, Yang CM, Yang CH. Combined quantitative and qualitative optical coherence tomography angiography

- biomarkers for predicting active neovascular age-related macular degeneration. *Sci Rep* 2021; **11**: 18068 [PMID: 34508170 DOI: 10.1038/s41598-021-97652-2]
- 2 **Song P**, Du Y, Chan KY, Theodoratou E, Rudan I. The national and subnational prevalence and burden of age-related macular degeneration in China. *J Glob Health* 2017; **7**: 020703 [PMID: 29302323 DOI: 10.7189/jogh.07.020703]
 - 3 **Spaide RF**, Jaffe GJ, Sarraf D, Freund KB, Sadda SR, Staurengi G, Waheed NK, Chakravarthy U, Rosenfeld PJ, Holz FG, Souied EH, Cohen SY, Querques G, Ohno-Matsui K, Boyer D, Gaudric A, Blodi B, Baurnal CR, Li X, Coscas GJ, Brucker A, Singerman L, Luthert P, Schmitz-Valckenberg S, Schmidt-Erfurth U, Grossniklaus HE, Wilson DJ, Guymer R, Yannuzzi LA, Chew EY, Csaky K, Monés JM, Pauleikhoff D, Tadayoni R, Fujimoto J. Consensus Nomenclature for Reporting Neovascular Age-Related Macular Degeneration Data: Consensus on Neovascular Age-Related Macular Degeneration Nomenclature Study Group. *Ophthalmology* 2020; **127**: 616-636 [PMID: 31864668 DOI: 10.1016/j.ophtha.2019.11.004]
 - 4 **Thomas CJ**, Mirza RG, Gill MK. Age-Related Macular Degeneration. *Med Clin North Am* 2021; **105**: 473-491 [PMID: 33926642 DOI: 10.1016/j.mcna.2021.01.003]
 - 5 **Bakri SJ**, Thorne JE, Ho AC, Ehlers JP, Schoenberger SD, Yeh S, Kim SJ. Safety and Efficacy of Anti-Vascular Endothelial Growth Factor Therapies for Neovascular Age-Related Macular Degeneration: A Report by the American Academy of Ophthalmology. *Ophthalmology* 2019; **126**: 55-63 [PMID: 30077616 DOI: 10.1016/j.ophtha.2018.07.028]
 - 6 **Mettu PS**, Allingham MJ, Cousins SW. Incomplete response to Anti-VEGF therapy in neovascular AMD: Exploring disease mechanisms and therapeutic opportunities. *Prog Retin Eye Res* 2021; **82**: 100906 [PMID: 33022379 DOI: 10.1016/j.preteyeres.2020.100906]
 - 7 **Waldstein SM**, Simader C, Staurengi G, Chong NV, Mitchell P, Jaffe GJ, Lu C, Katz TA, Schmidt-Erfurth U. Morphology and Visual Acuity in Aflibercept and Ranibizumab Therapy for Neovascular Age-Related Macular Degeneration in the VIEW Trials. *Ophthalmology* 2016; **123**: 1521-1529 [PMID: 27157149 DOI: 10.1016/j.ophtha.2016.03.037]
 - 8 **Amoaku WM**, Chakravarthy U, Gale R, Gavin M, Ghanchi F, Gibson J, Harding S, Johnston RL, Kelly SP, Lotery A, Mahmood S, Menon G, Sivaprasad S, Talks J, Tufail A, Yang Y. Defining response to anti-VEGF therapies in neovascular AMD. *Eye (Lond)* 2015; **29**: 721-731 [PMID: 25882328 DOI: 10.1038/eye.2015.48]
 - 9 **Giorno P**, Iacono P, Scarinci F, Di Renzo A, Varano M, Parravano M. Microvasculature Changes of Myopic Choroidal Neovascularization and the Predictive Value of Feeder Vessel Disappearance after Ranibizumab Treatment Revealed Using Optical Coherence Tomography Angiography. *Ophthalmologica* 2020; **243**: 263-270 [PMID: 31838464 DOI: 10.1159/000504755]
 - 10 **Wang Y**, Sun J, Wu J, Jia H, Feng J, Chen J, Yan Q, Huang P, Wang F, Bo Q, Sun X. Growth of nonexudative macular neovascularization in age-related macular degeneration: an indicator of biological lesion activity. *Eye (Lond)* 2023; **37**: 2048-2054 [PMID: 36434285 DOI: 10.1038/s41433-022-02282-1]
 - 11 **Nakano Y**, Kataoka K, Takeuchi J, Fujita A, Kaneko H, Shimizu H, Ito Y, Terasaki H. Vascular maturity of type 1 and type 2 choroidal neovascularization evaluated by optical coherence tomography angiography. *PLoS One* 2019; **14**: e0216304 [PMID: 31034505 DOI: 10.1371/journal.pone.0216304]
 - 12 **Jia H**, Lu B, Zhao Z, Yu Y, Wang F, Zhou M, Sun X. Prediction of the short-term efficacy of anti-VEGF therapy for neovascular age-related macular degeneration using optical coherence tomography angiography. *Eye Vis (Lond)* 2022; **9**: 16 [PMID: 35505390 DOI: 10.1186/s40662-022-00287-1]
 - 13 **Al-Sheikh M**, Iafe NA, Phasukkijwatana N, Sadda SR, Sarraf D. BIOMARKERS OF NEOVASCULAR ACTIVITY IN AGE-RELATED MACULAR DEGENERATION USING OPTICAL COHERENCE TOMOGRAPHY ANGIOGRAPHY. *Retina* 2018; **38**: 220-230 [PMID: 28582276 DOI: 10.1097/IAE.0000000000001628]
 - 14 **Coscas F**, Lupidi M, Boulet JF, Sellam A, Cabral D, Serra R, François C, Souied EH, Coscas G. Optical coherence tomography angiography in exudative age-related macular degeneration: a predictive model for treatment decisions. *Br J Ophthalmol* 2019; **103**: 1342-1346 [PMID: 30467129 DOI: 10.1136/bjophthalmol-2018-313065]
 - 15 **Miere A**, Butori P, Cohen SY, Semoun O, Capuano V, Jung C, Souied EH. Vascular Remodeling of Choroidal Neovascularization After Anti-Vascular Endothelial Growth Factor Therapy Visualized on Optical Coherence Tomography Angiography. *Retina* 2019; **39**: 548-557 [PMID: 29210939 DOI: 10.1097/IAE.0000000000001964]
 - 16 **Coscas F**, Cabral D, Pereira T, Galdes C, Narotamo H, Miere A, Lupidi M, Sellam A, Papoila A, Coscas G, Souied E. Quantitative optical coherence tomography angiography biomarkers for neovascular age-related macular degeneration in remission. *PLoS One* 2018; **13**: e0205513 [PMID: 30300393 DOI: 10.1371/journal.pone.0205513]
 - 17 **Faatz H**, Rothaus K, Ziegler M, Book M, Spital G, Lange C, Lommatzsch A. The Architecture of Macular Neovascularizations Predicts Treatment Responses to Anti-VEGF Therapy in Neovascular AMD. *Diagnostics (Basel)* 2022; **12** [PMID: 36428867 DOI: 10.3390/diagnostics12112807]
 - 18 **Serra R**, Coscas F, Pinna A, Cabral D, Coscas G, Souied EH. Quantitative Optical Coherence Tomography Angiography Features of Inactive Macular Neovascularization in Age-Related Macular Degeneration. *Retina* 2021; **41**: 93-102 [PMID: 32281767 DOI: 10.1097/IAE.0000000000002807]
 - 19 **Carnevali A**, Cicinelli MV, Capuano V, Corvi F, Mazzaferro A, Querques L, Scordia V, Souied EH, Bandello F, Querques G. Optical Coherence Tomography Angiography: A Useful Tool for Diagnosis of Treatment-Naïve Quiescent Choroidal Neovascularization. *Am J Ophthalmol* 2016; **169**: 189-198 [PMID: 27394033 DOI: 10.1016/j.ajo.2016.06.042]
 - 20 **Dansingani KK**, Freund KB. Optical Coherence Tomography Angiography Reveals Mature, Tangled Vascular Networks in Eyes With Neovascular Age-Related Macular Degeneration Showing Resistance to Geographic Atrophy. *Ophthalmic Surg Lasers Imaging Retina* 2015; **46**: 907-912 [PMID: 26469229 DOI: 10.3928/23258160-20151008-02]
 - 21 **Iafe NA**, Phasukkijwatana N, Sarraf D. Optical Coherence Tomography Angiography of Type 1 Neovascularization in Age-Related Macular Degeneration. *Dev Ophthalmol* 2016; **56**: 45-51 [PMID: 27023719 DOI: 10.1159/000442776]
 - 22 **Kuehlewein L**, Sadda SR, Sarraf D. OCT angiography and sequential quantitative analysis of type 2 neovascularization after ranibizumab therapy. *Eye (Lond)* 2015; **29**: 932-935 [PMID: 25976641 DOI: 10.1038/eye.2015.80]
 - 23 **Farecki ML**, Gutfleisch M, Faatz H, Rothaus K, Heimes B, Spital G, Lommatzsch A, Pauleikhoff D. Characteristics of type 1 and 2 CNV in exudative AMD in OCT-Angiography. *Graefes Arch Clin Exp Ophthalmol* 2017; **255**: 913-921 [PMID: 28233061 DOI: 10.1007/s00417-017-3588-y]
 - 24 **Suzuki M**, Nagai N, Izumi-Nagai K, Shinoda H, Koto T, Uchida A, Mochimaru H, Yuki K, Sasaki M, Tsubota K, Ozawa Y. Predictive factors for non-response to intravitreal ranibizumab treatment in age-related macular degeneration. *Br J Ophthalmol* 2014; **98**: 1186-1191 [PMID: 24711658 DOI: 10.1136/bjophthalmol-2013-304670]

- 25 **Kuchlewein L**, Bansal M, Lenis TL, Iafe NA, Satta SR, Bonini Filho MA, De Carlo TE, Waheed NK, Duker JS, Sarraf D. Optical Coherence Tomography Angiography of Type 1 Neovascularization in Age-Related Macular Degeneration. *Am J Ophthalmol* 2015; **160**: 739-48.e2 [PMID: 26164826 DOI: 10.1016/j.ajo.2015.06.030]
- 26 **Daniel E**, Pan W, Ying GS, Kim BJ, Grunwald JE, Ferris FL 3rd, Jaffe GJ, Toth CA, Martin DF, Fine SL, Maguire MG; Comparison of Age-related Macular Degeneration Treatments Trials. Development and Course of Scars in the Comparison of Age-Related Macular Degeneration Treatments Trials. *Ophthalmology* 2018; **125**: 1037-1046 [PMID: 29454660 DOI: 10.1016/j.ophtha.2018.01.004]
- 27 **Daniel E**, Toth CA, Grunwald JE, Jaffe GJ, Martin DF, Fine SL, Huang J, Ying GS, Hagstrom SA, Winter K, Maguire MG; Comparison of Age-related Macular Degeneration Treatments Trials Research Group. Risk of scar in the comparison of age-related macular degeneration treatments trials. *Ophthalmology* 2014; **121**: 656-666 [PMID: 24314839 DOI: 10.1016/j.ophtha.2013.10.019]
- 28 **Arganda-Carreras I**, Fernández-González R, Muñoz-Barrutia A, Ortiz-De-Solorzano C. 3D reconstruction of histological sections: Application to mammary gland tissue. *Microsc Res Tech* 2010; **73**: 1019-1029 [PMID: 20232465 DOI: 10.1002/jemt.20829]



Published by **Baishideng Publishing Group Inc**
7041 Koll Center Parkway, Suite 160, Pleasanton, CA 94566, USA
Telephone: +1-925-3991568
E-mail: office@baishideng.com
Help Desk: <https://www.f6publishing.com/helpdesk>
<https://www.wjgnet.com>

